

Electroluminescence and multi-photon effects in a resonator driven by a tunnel junction

Jinshuang Jin,^{1,2,3} Michael Marthaler,³ and Gerd Schön^{1,3,4}

¹*Institute of Nanotechnology, Karlsruhe Institute of Technology (KIT), 76021 Karlsruhe, Germany*

²*Department of Physics, Hangzhou Normal University, Hangzhou 310036, China*

³*Institut für Theoretische Festkörperphysik, Karlsruhe Institute of Technology (KIT), 76131 Karlsruhe, Germany*

⁴*DFG Center for Functional Nanostructures, Karlsruhe Institute of Technology (KIT), 76131 Karlsruhe, Germany*

(Dated: February 29, 2024)

We consider a transmission line resonator which is driven by electrons tunneling through a voltage-biased tunnel junction. Using the Born-Markovian quantum master equation in the polaron basis we investigate the nonequilibrium photon state and emission spectrum of the resonator as well as properties of the transport current across the tunnel junction and its noise spectrum. The electroluminescence is optimized, with maximum peak height and narrow linewidth, when the back-action of the tunnel junction on the resonator and the decay rate of the resonator are similar in strength. For strong coupling between the resonator and tunnel junction, multi-photon effects show up in the noise spectrum of the transport current.

PACS numbers: 85.60.-q, 73.23.-b, 73.63.Rt, 72.70.+m

I. INTRODUCTION

Circuit quantum electrodynamics (cQED) of on-chip solid-state systems coupled to a microwave resonator has attracted much attention. The investigations were stimulated by the possibility of strong coupling between a superconducting qubit and a transmission line resonator¹⁻³. This allowed demonstrating phenomena known from quantum optics in the solid-state systems with unprecedented quality. Some of the examples are vacuum Rabi splitting^{2,3}, further advanced applications of quantum state engineering⁴⁻⁶, as well as single-qubit lasing and cooling⁷⁻⁹.

The development of cQED is not restricted to superconducting systems but has also been extended to solid-state devices composed of gate-defined semiconductor quantum dots or multi-dot systems coupled to resonators¹⁰⁻¹⁶. Of particular interest is the interplay of the electrons tunneling through the dots and the excitation of photons in the resonator. Single electron tunneling through a double dot setup can produce a population inversion and induce a lasing state in the electromagnetic resonator^{10,11}, which is accompanied by pronounced features such as super- or sub-Poissonian noise of the transport current¹⁶. For a simpler system, a resonator driven by electrons tunneling through a single quantum dot, the nonequilibrium photon population has also been investigated¹³.

Continuing to even more basic systems, the question arises, what is the nonequilibrium photon state created in the resonator by electrons tunneling across a single junction without intermediate quantum dots. Recently, such a system has been investigated experimentally, and the resonator was found to influence the finite-frequency shot-noise of the transport current through the junction similar as a thermal electromagnetic environment¹⁷. A study of nonequilibrium effects in the resonator which is

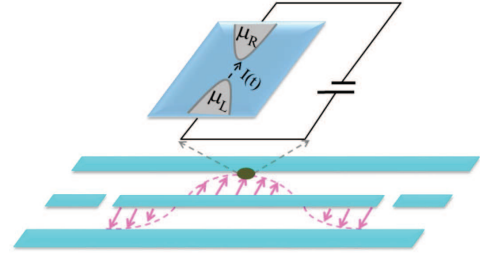


FIG. 1: (Color online) Schematic view of a tunnel junction-resonator circuit. The junction is placed at a maximum of the electric field of the transmission line resonator in order to maximize the dipole interaction.

strongly coupled to a biased tunnel junction has, to the best of our knowledge, not yet been performed, although the setup may find wide applications. For instance, the system has been used as an effective charge detector for single-shot read-out of quantum-dot based qubits¹⁸⁻²¹, and as a displacement detector which can resolve the momentum and position of nanomechanical resonators with high precision²²⁻²⁶. Recently, it has been proposed that a tunnel junction can be used to generate squeezed light and microwave photon pairs^{27,28}.

In this work we study the nonequilibrium photon state in a transmission line resonator which is strongly coupled to the electrons tunneling through a tunnel junction (TJ). We focus on the electroluminescence of the excited photons in the driven resonator, as well as the transport current through the tunnel junction and its noise spectrum. In Sec. II, we introduce the model of the TJ-resonator circuit and present the quantum master equation describing the dynamics of the coupled system. We investigate the system in Sec. III for moderately strong coupling, where single-photon processes dominate the dynamics. In this limit we find analytic results. We then study numerically in Sec. IV multi-photon effects

which get visible in what is called the ultra-strong coupling limit. We conclude with a summary.

II. METHODOLOGY

A. The system

We consider a superconducting transmission line resonator strongly coupled to a tunnel junction in a setup as sketched in Fig. 1. The corresponding Hamiltonian is given by ($\hbar = 1$),

$$H_{\text{tot}} = \sum_{\alpha k} \varepsilon_{\alpha k} c_{\alpha k}^\dagger c_{\alpha k} + \sum_{kk'} (t_{kk'} c_{Lk}^\dagger c_{Rk'} + \text{H.c.}) + \omega_r a^\dagger a + g \sum_k (c_{Rk}^\dagger c_{Rk} - c_{Lk}^\dagger c_{Lk})(a + a^\dagger). \quad (1)$$

The first line describes the tunnel junction between the left and right ($\alpha = L, R$) reservoirs with single-particle energies $\varepsilon_{\alpha k}$ and tunneling amplitudes $t_{kk'}$ between the two reservoirs. The resonator is modeled by a harmonic oscillator with frequency ω_r . The coupling of the two subsystems with strength g is assumed to be induced by the electric field of the resonator across the tunnel junction, as illustrated in Fig. 1, which shifts the chemical potentials of the two reservoirs. We assume shifts of equal strength for both sides, but the generalization would be straightforward.

We proceed using the polaron transformation, $\tilde{H} = U H U^\dagger$ with $U = \exp[\frac{g}{\omega_r} \sum_k (c_{Rk}^\dagger c_{Rk} - c_{Lk}^\dagger c_{Lk})(a^\dagger - a)]$. It transforms the Hamiltonian (1) to

$$\tilde{H}_{\text{tot}} = \sum_{\alpha k} \varepsilon_{\alpha k} c_{\alpha k}^\dagger c_{\alpha k} + \omega_r a^\dagger a + \sum_{kk'} (t_{kk'} c_{Lk}^\dagger c_{Rk'} e^{-\lambda(a^\dagger - a)} + \text{H.c.}). \quad (2)$$

Here we neglected a trivial energy shift in the electrodes and introduced the dimensionless coupling strength $\lambda \equiv 2g/\omega_r$. In the interaction picture with respect to the reservoir $H_B = \sum_{\alpha k} \varepsilon_{\alpha k} c_{\alpha k}^\dagger c_{\alpha k}$, we recast the Hamiltonian (2) as $\tilde{H}_{\text{tot}}(t) = H_r + H'(t)$ with $H_r = \omega_r a^\dagger a$ and coupling

$$H'(t) = F^\dagger(t) Q + Q^\dagger F(t). \quad (3)$$

The operator of the tunnel junction is $F^\dagger(t) = \sum_{kk'} t_{kk'} c_{Lk}^\dagger c_{Rk'} e^{i\Delta_{kk'} t}$ with $\Delta_{kk'} = \varepsilon_{Lk} - \varepsilon_{Rk'}$, while $Q = \exp[-\lambda(a^\dagger - a)]$ refers to the resonator. For later use we introduce the correlation functions of the bath accounting for forward (L to R) and backward tunneling, $C^{(+)}(t) \equiv \langle F^\dagger(t) F(0) \rangle_B$ and $C^{(-)}(t) \equiv \langle F(t) F^\dagger(0) \rangle_B$, respectively. Here $\langle \dots \rangle_B$ stands for the statistical average over both electron reservoirs. They are assumed to be in thermal equilibrium, in which case the correlators reduce to

$$C^{(\pm)}(t) = \sum_{kk'} e^{\pm i\Delta_{kk'} t} |t_{kk'}|^2 f_{Lk}^\pm f_{Rk'}^\mp. \quad (4)$$

Here we introduced the Fermi-Dirac function of the α -lead $f_{\alpha k}^\pm \equiv f_{\alpha k} = [e^{\beta(\varepsilon_{\alpha k} - \mu_\alpha)} + 1]^{-1}$ with $\beta = 1/(k_B T)$ and $f_{\alpha k}^- = 1 - f_{\alpha k}$. We focus on the limit of a tunnel junction, where the tunneling probabilities of each channel are much smaller than unity, and we assume momentum-independent tunneling amplitudes $t_{kk'} = t$. In combination with the densities of states ν_α of the α -reservoir they determine the tunneling resistance R and the dimensionless tunneling strength $\eta = 1/(2e^2 R) = \pi |t|^2 \nu_L \nu_R$. We assume $\eta \ll 1$ to be small. The bath correlators in Fourier space $\tilde{C}^{(\pm)}(\omega) = \int_{-\infty}^{\infty} dt e^{i\omega t} C^{(\pm)}(t)$ thus become

$$\tilde{C}^{(\pm)}(\omega) = \frac{2\eta(\omega \pm eV)}{1 - e^{-\beta(\omega \pm eV)}}. \quad (5)$$

They account for forward and backward tunneling processes with energy absorption ($\omega > 0$) and emission ($\omega < 0$). Here $eV = \mu_L - \mu_R$ is the applied bias voltage across the tunnel junction.

B. Quantum Master Equation

Starting from the total density operator $\rho_{\text{tot}}(t)$ of the combined TJ-resonator system one obtains the reduced density matrix of the resonator by tracing out the bath degrees of freedom of the two electronic reservoirs, $\rho(t) = \text{tr}_B[\rho_{\text{tot}}(t)]$. Treating $H'(t)$ as perturbation and expanding up to second-order leads to the Born-Markovian master equation

$$\dot{\rho}(t) = -i[H_r, \rho(t)] + \mathcal{L}_\kappa \rho(t) + \mathcal{L}_B \rho(t) \equiv \mathcal{L} \rho(t). \quad (6a)$$

While the first term describes the coherent evolution, the second is the standard decay term of the resonator with the decay rate κ , and the third term accounts for the effect of the tunnel junction. They are given by

$$\begin{aligned} \mathcal{L}_\kappa \rho &= \kappa(n_{\text{th}} + 1) [a \rho a^\dagger - \frac{1}{2}(a^\dagger a \rho + \rho a^\dagger a)] + \\ &+ \kappa n_{\text{th}} [a^\dagger \rho a - \frac{1}{2}(a a^\dagger \rho + \rho a a^\dagger)], \end{aligned} \quad (6b)$$

$$\begin{aligned} \mathcal{L}_B \rho &= \frac{1}{2} \left(\tilde{Q}_- \rho Q^\dagger + Q \rho \tilde{Q}_-^\dagger - Q^\dagger \tilde{Q}_- \rho - \rho \tilde{Q}_-^\dagger Q \right. \\ &\left. + \tilde{Q}_+^\dagger \rho Q + Q^\dagger \rho \tilde{Q}_+ - Q \tilde{Q}_+^\dagger \rho - \rho \tilde{Q}_+ Q^\dagger \right). \end{aligned} \quad (6c)$$

Here $n_{\text{th}} = [\exp(\beta\omega_r) - 1]^{-1}$ is the thermal photon number in the resonator, and we introduced the operators

$$\tilde{Q}_\pm = \int_{-\infty}^{\infty} dt C^{(\pm)}(t) e^{\pm i H_r t} Q e^{\mp i H_r t}.$$

The further calculations are done in the basis of Fock states, $H_r |n\rangle = n\omega_r |n\rangle$, of the photons in the resonator, for which the operator entering the coupling Eq. (3) is expressed as $Q = \sum_{nm} Q_{mn} |m\rangle \langle n|$ $Q_{mn} = \langle m | e^{-\lambda(a^\dagger - a)} | n \rangle$. Correspondingly, the elements of the operator \tilde{Q}_\pm are calculated via $\langle m | \tilde{Q}_\pm | n \rangle =$

$\tilde{C}^{(\pm)}(\pm\omega_{mn})Q_{mn}$, with $\omega_{mn} \equiv (m - n)\omega_r$ and $\tilde{C}^{(\pm)}(\pm\omega_{mn})$ given by Eq. (5). Based on this master equation, the emission spectrum of the resonator,

$$S_r(\omega) \equiv \lim_{t \rightarrow \infty} \int_{-\infty}^{\infty} d\tau \langle a^\dagger(t)a(t+\tau) \rangle e^{i\omega\tau}, \quad (7)$$

as well as the second-order correlation function in the stationary limit $g^{(2)}(\tau) = \lim_{t \rightarrow \infty} \langle a^\dagger(t)a^\dagger(t+\tau)a(t+\tau)a(t) \rangle / \langle a^\dagger(t)a(t) \rangle^2$, can be calculated via the quantum regression theorem²⁹.

Starting from $I(t) = -e d\langle n_R(t) \rangle / dt$ with $n_R = \sum_k c_{Rk}^\dagger c_{Rk}$ we obtain the transport current³⁰ $I(t) = \langle \hat{I}(t) \rangle = \text{Tr}[\hat{I}\rho(t)]$ with current operators

$$\hat{I}\rho(t) = \frac{e}{2} [Q^\dagger \rho(t) \tilde{Q}_+ - \tilde{Q}_- \rho(t) Q^\dagger + \text{H.c.}]. \quad (8)$$

From this we calculate the average current $I(t)$ and the current noise spectrum

$$S_I(\omega) = \int_{-\infty}^{\infty} dt \langle \{\delta \hat{I}(t), \delta \hat{I}(0)\} \rangle e^{i\omega t}, \quad (9)$$

with $\delta \hat{I}(t) = \hat{I}(t) - I$. The noise spectrum can again be calculated using the quantum regression theorem.

In the present work we consider a high-quality resonator with Q factor assumed to be 2×10^4 , corresponding to a decay rate $\kappa = 5 \times 10^{-5}\omega_r$. It is much smaller than both the tunneling rate and coupling strength, i.e., $\kappa/\omega_r \ll \eta, \lambda$.

III. MODERATE COUPLING STRENGTH

For weak to moderate coupling strength $\lambda \ll 1$ (but still $\kappa/\omega_r \ll \lambda$) we proceed in an expansion up to 2nd order, i.e. $Q = e^{-\lambda(a^\dagger - a)} \approx 1 - \lambda(a^\dagger - a) + \frac{1}{2}\lambda^2(a^\dagger - a)^2$. For definiteness we assume low temperatures, where the electrons tunnel only from the left to the right lead without the reverse process, and the number of thermal photons in the resonator vanishes, $n_{\text{th}} = 0$. In this case the quantum master equation for the oscillator reduces to

$$\begin{aligned} \dot{\rho} = & -i[H_r, \rho(t)] + (\kappa + \Gamma_+) [a\rho a^\dagger - \frac{1}{2}(a^\dagger a\rho + \rho a^\dagger a)] \\ & + \Gamma_- [a^\dagger \rho a - \frac{1}{2}(aa^\dagger \rho + \rho aa^\dagger)], \end{aligned} \quad (10)$$

with rates $\Gamma_\pm = \lambda^2 \tilde{C}^{(+)}(\pm\omega_r)$. In the considered limit we could make use of the rotating wave approximation. The resulting master equation (10) accounts for single-photon processes, i.e. processes where electrons tunneling through the junction are associated with the emission or absorption of a single photon in the resonator with rates Γ_- and Γ_+ , respectively. Interestingly, the second order term of the expansion of Q does not modify the master equation, however, it does modify the average current to be studied later.

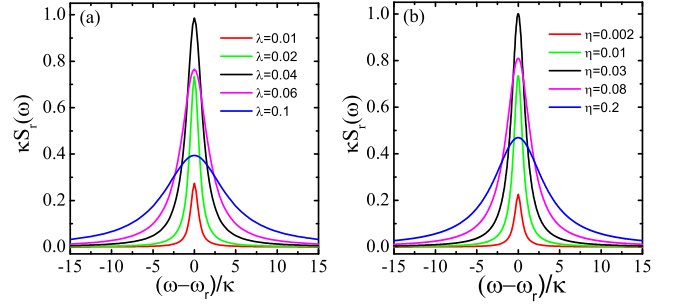


FIG. 2: (Color online) The emission spectrum of the resonator $S_r(\omega)$ near the one-photon resonance, (a) for $\eta = 0.01$ and different coupling strengths and (b) for $\lambda = 0.02$ and different tunneling rates. The other parameters are: low temperature $k_B T = 0.02\omega_r$ and bias voltage $eV = 3\omega_r$.

From Eq. (10) we see that the resonator is subject to an effective decay rate³¹

$$\kappa_{\text{eff}} = \Gamma_+ - \Gamma_- + \kappa \approx 4\eta\lambda^2\omega_r + \kappa, \quad (11)$$

and the average photon number is

$$\bar{n} = \frac{\Gamma_-}{\Gamma_+ - \Gamma_- + \kappa} \approx \frac{\eta\lambda^2(eV - \omega_r)}{2\eta\lambda^2\omega_r + \kappa/2} \Theta(eV - \omega_r). \quad (12)$$

Here, Θ is the step function, $\bar{n} = \langle a^\dagger a \rangle = \sum_n n P_n$ with $P_n = \rho_{nn}$. The corresponding photon distribution, $P_n \approx \langle n \rangle^n / (1 + \langle n \rangle)^{n+1}$ coincides with a Bose-Einstein distribution with effective temperature

$$k_B T_{\text{eff}} \approx \omega_r / \ln \left[\frac{\eta\lambda^2(eV + \omega_r) + \kappa/2}{\eta\lambda^2(eV - \omega_r)} \right] \Theta(eV - \omega_r).$$

This result coincides with the intensity distribution of classical chaotic light^{32,33}. A similar result has been obtained in Ref. 13 for a resonator driven by electrons tunneling through a single quantum dot.

For the second-order correlation function we get

$$g^{(2)}(\tau) = 1 + e^{-\kappa_{\text{eff}}\tau}. \quad (13)$$

It displays bunching, $g^{(2)}(0) = 2$, for vanishing delay time and approaches $g^{(2)}(\tau \rightarrow \infty) = 1$ for long delay time, when no correlations exist between the excited photons.

From the master equation we further get the emission spectrum of the resonator,

$$S_r(\omega) = \frac{\kappa_{\text{eff}} \bar{n}}{(\omega_r - \omega)^2 + (\kappa_{\text{eff}}/2)^2}. \quad (14)$$

Results are shown in Fig. 2. With increasing coupling strength λ , or tunneling strength η , the height of the peak first increases and then decreases with simultaneous broadening of the linewidth. The maximum height of the peak at $\omega = \omega_r$ is

$$S_r(\omega_r) = \frac{4\bar{n}}{\kappa_{\text{eff}}} \approx \frac{2\eta\lambda^2(eV - \omega_r)}{(2\eta\lambda^2\omega_r + \kappa/2)^2} \Theta(eV - \omega_r). \quad (15)$$

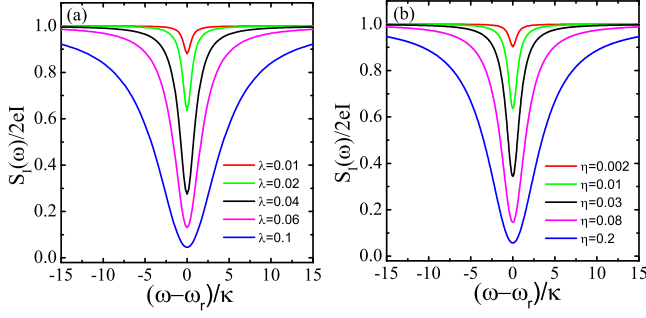


FIG. 3: (Color online) The noise spectrum of the transport current through the junction $S_I(\omega)$, (a) for $\eta = 0.01$ and different coupling strengths and (b) for $\lambda = 0.02$ and different tunneling rates. The other parameters are the same as in Fig. 2.

When the parameters satisfy the relation

$$\eta_p \lambda_p^2 = \frac{\kappa}{4\omega_r}, \quad (16)$$

the peak height is largest, with $S_r^{\max}(\omega_r) = (eV - \omega_r)\Theta(eV - \omega_r)/(2\kappa\omega_r)$, while the linewidth is still narrow, $(\kappa_{\text{eff}})_p/2 = \kappa$. This means that we find an optimal electroluminescence when the dissipative rate induced by the tunnel junction ($4\eta\lambda^2\omega_r$) is similar to the decay rate of the resonator (κ).

In the considered limit (i.e., up to λ^2) we get from Eq. (8) and Eq. (9) the average current,

$$I = (1 - \lambda^2)\tilde{C}^{(+)}(0) + \lambda^2\tilde{C}^{(+)}(-\omega_r) \approx 2\eta(1 - \lambda^2)eV + 2\eta\lambda^2(eV - \omega_r)\Theta(eV - \omega_r), \quad (17)$$

and the current noise spectrum around $\omega = \pm\omega_r$,

$$S_I(\omega) \approx 2eI + \sum_{+,-} \frac{c_1\kappa_{\text{eff}}/2}{(\omega \pm \omega_r)^2 + (\kappa_{\text{eff}}/2)^2} \Theta(eV - \omega_r), \quad (18)$$

with the coefficient $c_1 = -8e\eta^2\lambda^2\omega_r[eV + (\bar{n} - 1/2)\omega_r]$. Below the onset of single-photon processes the transport current is suppressed by the coupling to the resonator. This effect is described by the Franck-Condon factor which renormalizes the tunneling rate¹³, by a factor $(1 - \lambda^2/2)^2$. Above the threshold, when photons can be exited the current grows as described by the second term. The noise spectrum further demonstrates the interplay of electrons tunneling through the junction with the emission and absorption of photons in the resonator. This combination leads to a dip in the spectrum, shown in Fig. 3, at $\omega = \pm\omega_r$. The dip gets deeper, i.e. $|S(\omega_r) - 2eI| \approx 2|c_1|/\kappa_{\text{eff}}$ increases, with growing coupling or tunneling strengths. The corresponding linewidth, κ_{eff} (ω is consistent with that of the emission spectrum.

A comparison with the numerical solution of the full problem, presented in the following section, shows that analytic results obtained so far for weak to moderate coupling strength are valid as long as $\lambda \lesssim 0.2$.

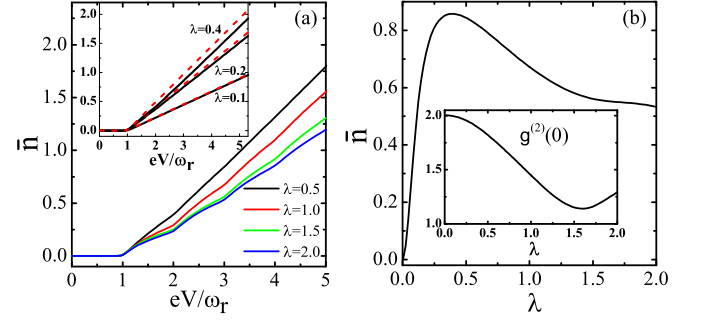


FIG. 4: (Color online) The average number of photons excited in the resonator (a) as a function of the bias voltage (eV) and (b) as a function of the coupling strength (λ) with $eV = 3\omega_r$ at low temperature $k_B T = 0.02\omega_r$ and tunneling rate $\eta = 0.001$. The insets in (a) is for moderate coupling strength based on the exact numerical calculation (solid-line) and analytical expression of Eq. (12) (dashed-line). It is sufficient only for $\lambda \lesssim 0.2$.

IV. ULTRASTRONG COUPLING

We turn now to the so-called ultrastrong-coupling regime where the coupling strength between tunnel junction and resonator is of the order of the resonator frequency. Values which we consider realistic, and for which the present method is valid, are $0.1\omega_r < g \lesssim \omega_r$ (i.e., $0.2 < \lambda = 2g/\omega_r \lesssim 2$). Although more difficult to realize in an experiment, this limit displays interesting new properties.

In this regime, the single-photon approximation obtained from an expansion up to order λ^2 and analyzed in Sec. III, is no longer sufficient. Instead two- and multi-photon processes associated with the excitations of multiple photons which follow from expanding $Q = e^{-\lambda(a^\dagger - a)}$ to higher orders in λ get important. In order to study these processes we solved the equations introduced above numerically without further approximations. In contrast to the single-photon limit, the average photon number, as shown in Fig. 4, in general depends nonlinearly on the bias voltage and even decreases with increasing coupling strength. The nonequilibrium photon state is similar to that found when the resonator is driven by electrons tunneling through a single quantum dot, studied in Ref. 13. The state of the photons in the resonator deviates from a thermal state. E.g., as shown in the inset of Fig. 4 (b) the second-order correlation function deviates from the value $g_{\text{thermal}}^{(2)}(0) = 2$ which we would find for a thermal (chaotic) state.

The effect of the multi-photon processes on the transport current becomes significant with increasing coupling strength and manifests itself in a nonlinear-dependence on the bias voltage as shown in Fig. 5 (a). Simultaneously, the multi-photon effects enhance the current fluctuations and induce the super-Poissonian behavior in the zero-frequency shot noise shown in Fig. 6 (a). The multi-photon effects can also be observed in the current noise

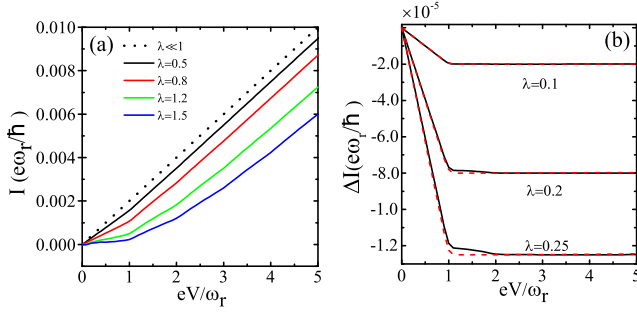


FIG. 5: (Color online) The average current tunneling through the junction as a function of the bias voltage for different coupling strength. Multi-photon effect becomes significant with increasing coupling strength shown in (a). (b) displays the effect of the resonator on the transport current, i.e., $\Delta I = I - I_0$ with $I_0 = 2\eta eV$, for moderate coupling strength based on the exact formula of Eq. (8) (solid-line) and analytical expression of Eq. (17) (dashed-line). The other parameters are the same as in Fig. 4

spectrum. In an expansion up to fourth order in the coupling we obtain the noise spectrum near $\omega = 0$ and $\omega = \pm 2\omega_r$,

$$S_I(\omega) \propto e\eta^2 \lambda^4 \left[\frac{c_0 \kappa_{\text{eff}}}{\omega^2 + \kappa_{\text{eff}}^2} + \sum_{+,-} \frac{c_2 \kappa_{\text{eff}}}{(\omega \pm 2\omega_r)^2 + \kappa_{\text{eff}}^2} \right],$$

with positive coefficients $c_0 > 0$ and $c_2 > 0$. The two-photon processes lead to peaks in the noise spectrum at $\omega = 0$ and $\omega = \pm 2\omega_r$ with linewidth determined by κ_{eff} , as shown in Fig. 6 (a) and (c). Compared to the dip at $\omega = \omega_r$, the peaks at $\omega = 0$ and $\omega = \pm 2\omega_r$ are more sensitive to the coupling strength, as the comparison of Figs. 6(a), (b), and (c) demonstrates. Three-photon effects, which we find by expanding further, lead again to a dip in the noise spectrum at $\omega = \pm 3\omega_r$, as shown in Fig. 6 (d), with properties similar to the one-photon signal. We expect that the noise spectrum shows alternating dips and peaks for odd- (at $\omega = (2n+1)\omega_r$) and even-photon-number processes (at $\omega = 2n\omega_r$, $n = 0, 1, 2, \dots$), respectively.

V. SUMMARY

In summary, we have investigated the hybrid system of a transmission line resonator strongly coupled to a tunnel junction. The study is based on a Born-Markov master equation in the polaron limit, which accounts for the nonequilibrium state of the resonator. We presented results for two regimes of coupling strength between resonator and tunnel junction, characterized by single photon- or multiple photon-processes, respectively.

For weak to moderate coupling, i.e., in the single-photon limit, we obtained analytical results at low temperatures for both the average number of the excited

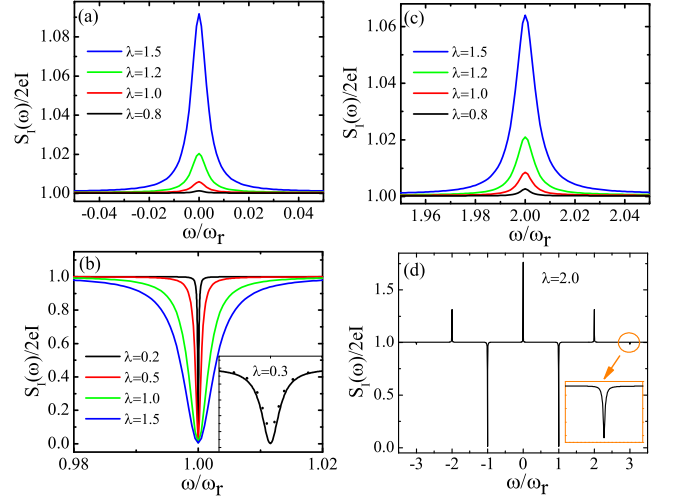


FIG. 6: (Color online) The noise spectrum of the transport current through the tunnel junction for ultrastrong-coupling (a) around zero-frequency, (b) for single-photon, (c) two-photon, and (d) generally many-photon processes, respectively. The dotted line in the insets of (c) is obtained in the weak/moderate coupling approximation Eq. (18). It well describes the single-photon process in the noise spectrum showing the dip behavior at $\omega = \omega_r$ for $\lambda \lesssim 0.2$. The other parameters are the same as in Fig. 4.

photons and the average current with threshold behavior once the bias voltage allows the excitation of photons. The photon distribution can be parametrized by a thermal one with an enhanced effective temperature. For the electroluminescence of the resonator we found the optimal conditions, with maximum height of the peak and still narrow linewidth, when the resonator damping due to the tunnel junction is comparable in strength to the intrinsic decay rate of the resonator. The current noise spectrum shows a pronounced dip at the resonator frequency. These phenomena could be easily tested, since all the parameters are within reach of current experiments^{2,12,14,17,27,28,34}.

In the ultrastrong-coupling regime, multi-photon effects can be observed. The effect of the tunnel junction on the resonator can no longer be described by an effective heating. The average number of photons excited in the resonator, which first increases, eventually even decreases with increasing coupling strength. The multi-photon effects are most pronounced in the noise spectrum of the transport current in the junction. In addition to the dips at $\omega = \pm\omega_r$, it shows peaks and dips at $\omega = \pm 2\omega_r$ and $\omega = \pm 3\omega_r$ and so forth due to the interplay of the electrons tunneling through the junction associated with the emission and absorption of two-photons and three-photons in the resonator, respectively. The current voltage characteristic shows threshold behavior at voltages eV taking values which are multiples of the resonator frequency. While least spectacular this effect might be most easily observed in experiments.

Acknowledgments

We acknowledge stimulating discussions with K. Ensslin, T. Ihn, A. Wallraff, X.Q. Li, Y.J. Yan, P.-Q. Jin,

D. Golubev and Andreas Heimes. JSJ acknowledges support by a fellowship of the KIT, as well as the support in the Program of HNUET, and the NNSF of China (No.11274085).

-
- ¹ A. Blais, R.-S. Huang, A. Wallraff, S. M. Girvin, and R. J. Schoelkopf, *Phys. Rev. A* **69**, 062320 (2004).
 - ² A. Wallraff, D. I. Schuster, A. Blais, L. Frunzio, J. M. R. S. Huang, S. Kumar, S. M. Girvin, and R. J. Schoelkopf, *Nature* **431**, 162 (2004).
 - ³ I. Chiorescu, P. Bertet, K. Semba, Y. Nakamura, C. J. P. M. Harmans, and J. E. Mooij, *Nature* **431**, 159 (2004).
 - ⁴ J. Majer, J. M. Chow, J. M. Gambetta, J. Koch, B. R. Johnson, J. A. Schreier, L. Frunzio, D. I. Schuster, A. A. Houck, A. Wallraff, et al., *Nature* **449**, 443 (2007).
 - ⁵ M. A. Sillanpää, J. I. Park, and R. W. Simmonds, *Nature* **449**, 438 (2007).
 - ⁶ M. Hofheinz, H. Wang, M. Ansmann, R. C. Bialczak, E. Lucero, M. Neeley, A. D. O'Connell, D. Sank, J. Wenner, J. M. Martinis, et al., *Nature* **459**, 546 (2009).
 - ⁷ O. Astafiev, K. Inomata, A. O. Niskanen, T. Yamamoto, Y. A. Pashkin, Y. Nakamura, and J. S. Tsai, *Nature* **449**, 588 (2007).
 - ⁸ J. Hauss, A. Fedorov, C. Hutter, A. Shnirman, and G. Schön, *Phys. Rev. Lett.* **100**, 037003 (2008).
 - ⁹ M. Grajcar, S. H. W. van der Ploeg, A. Izmailkov, H. G. M. E. Ilichev, A. Fedorov, A. Shnirman, and G. Schön, *Nature Physics* **4**, 612 (2008).
 - ¹⁰ L. Childress, A. S. Sørensen, and M. D. Lukin, *Phys. Rev. A* **69**, 042302 (2004).
 - ¹¹ P.-Q. Jin, M. Marthaler, J. H. Cole, A. Shnirman, and G. Schön, *Phys. Rev. B* **84**, 035322 (2011).
 - ¹² T. Frey, P. J. Leek, M. Beck, K. Ensslin, A. Wallraff, and T. Ihn, *Applied Physics Letters* **98**, 262105 (2011).
 - ¹³ C. Bergenfeldt and P. Samuelsson, *Phys. Rev. B* **85**, 045446 (2012).
 - ¹⁴ T. Frey, P. J. Leek, M. Beck, A. Blais, T. Ihn, K. Ensslin, and A. Wallraff, *Phys. Rev. Lett.* **108**, 046807 (2012).
 - ¹⁵ M. R. Delbecq, V. Schmitt, F. D. Parmentier, N. Roch, J. J. Viennot, G. Fève, B. Huard, C. Mora, A. Cottet, and T. Kontos, *Phys. Rev. Lett.* **107**, 256804 (2011).
 - ¹⁶ J. Jin, M. Marthaler, P.-Q. Jin, D. Golubev, and G. Schön, *New Journal of Physics* **15**, 025044 (2013).
 - ¹⁷ C. Altimiras, O. Parlavacchio, P. Joyez, D. Vion, P. Roche, D. Esteve, and F. Portier, *Phys. Rev. Lett.* **112**, 236803 (2014).
 - ¹⁸ S. A. Gurvitz, *Phys. Rev. B* **56**, 15215 (1997).
 - ¹⁹ A. N. Korotkov, *Phys. Rev. B* **63**, 115403 (2001).
 - ²⁰ J. M. Elzerman, R. Hanson, L. H. Willems van Beveren, B. Witkamp, L. M. K. Vandersypen, and L. P. Kouwenhoven, *Nature* **430**, 431 (2004).
 - ²¹ T. Fujisawa, T. Hayashi, R. Tomita, and Y. Hirayama, *Nature* **312**, 1634 (2006).
 - ²² A. A. Clerk and S. M. Girvin, *Phys. Rev. B* **70**, 121303 (2004).
 - ²³ M. Poggio, M. P. Jura, C. L. Degen, M. A. Topinka, H. J. Mamin, D. Goldhaber-Gordon, and D. Rugar, *Nat. Phys.* **4**, 635 (2008).
 - ²⁴ J. Stettenheim, M. Thalakulam, F. Pan, M. Bal, Z. Ji, W. Xue, L. Pfeiffer, K. W. West, M. P. Blencowe, and A. J. Rimberg, *Nature Letters* **466**, 86 (2010).
 - ²⁵ S. Walter and B. Trauzettel, *Phys. Rev. B* **83**, 155411 (2011).
 - ²⁶ L. L. Benatov and M. P. Blencowe, *Phys. Rev. B* **86**, 075313 (2012).
 - ²⁷ G. Gasse, C. Lupien, and B. Reulet, *Phys. Rev. Lett.* **111**, 136601 (2013).
 - ²⁸ J.-C. Forgues, C. Lupien, and B. Reulet, eprint p. arXiv:1403.5578 (2014).
 - ²⁹ M. Scully and M. S. Zubairy, *Quantum Optics* (Cambridge University Press, Cambridge, 1997).
 - ³⁰ X. Q. Li, J. Y. Luo, Y. G. Yang, P. Cui, and Y. J. Yan, *Phys. Rev. B* **71**, 205304 (2005).
 - ³¹ H. J. Carmichael, *An Open System Approach to Quantum Optics* (Spring-Verlag, Berlin, 1993).
 - ³² R. Loudon, *The Quantum Theory of Light* (Clarendon, Oxford, 1983), 2nd ed.
 - ³³ H. P. Breuer and F. Petruccione, *The Theory of Open Quantum Systems* (Oxford University Press, Oxford, 2002).
 - ³⁴ N. Ubbelohde, C. Fricke, C. Flindt, F. Hohls, and R. J. Haug, *Nature Communications* **91**, 1 (2012).